


## Research Article

# The Effects of Branch Spacing and Number on the Uplift Bearing Capacity of a New Squeezed Multiple-Branch Pile: A Numerical Simulation Analysis

Qingqing Su<sup>1,2,3</sup> , Hongbing Xia,<sup>3</sup> Kunming Wu,<sup>1,2</sup> and Fulian Yang<sup>2</sup>

<sup>1</sup>Anhui Province Key Laboratory of Building Structure and Underground Engineering, Anhui Jianzhu University, Hefei, Anhui 230601, China

<sup>2</sup>School of Architecture and Civil Engineering, West Anhui University, Lu'an, 237000 Anhui, China

<sup>3</sup>School of Civil Engineering and Architecture, Anhui University of Science and Technology, Huainan, 232001 Anhui, China

Correspondence should be addressed to Qingqing Su; [qqsuhn@126.com](mailto:qqsuhn@126.com)

Received 20 November 2022; Revised 5 March 2023; Accepted 8 March 2023; Published 13 April 2023

Academic Editor: Giulia Pascoletti

Copyright © 2023 Qingqing Su et al. This is an open access article distributed under the Creative Commons Attribution License, which permits unrestricted use, distribution, and reproduction in any medium, provided the original work is properly cited.

The squeezed multiple-branch pile is a variable section pile that was built by adding a bearing branch cavity to a constant section pile using expansion and extrusion equipment. It is widely used in engineering practice for its high bearing capacity, small settlement deformation, high economic benefits, strong adaptability, and simple pile forming process. In this paper, a new type of squeezed multiple-branch pile is proposed and its forming tool is invented. The forming tool of the pile has applied for an invention patent and is authorized by the China National Intellectual Property Administration. Multiple groups of comparison models of the new squeezed multiple-branch piles are established by using FLAC3D numerical simulation software to investigate the influence of the number and spacing of branches on the bearing mechanism in response to uplift load. The results indicated that the number and spacing of branches have a significant effect on the uplift bearing capacity, load-displacement curves, side friction resistance, and stress distribution law in the new pile and soil around the pile. The suitable number and spacing of branches maximize the uplift bearing capacity and minimize the settlement of a single pile.

## 1. Introduction

A pile with multiple branches is a kind of variable section pile formed by adding bearing branches on the basis of a constant section pile. Compared with constant section piles [1], the bearing mechanism of the pile with multiple branches has changed greatly. The branch increases the action range of pile-soil and improves the pile-side friction. The branch enhances the effect of pile-soil interaction by making full use of the mechanical properties of each layer of soil between the branches. Hence, the bearing capacity of the single square concrete of the pile is significantly improved, so as to save on cost and shorten the construction period [2, 3].

Numerous researchers have devoted considerable vigor to the bearing capacity of the variable section pile and constant section pile via laboratory and in situ experiments, theoretical

analyses, and numerical simulation techniques. Numerous studies have been conducted to explore the soil-pile interaction mechanism and influence factors of bearing capacity for the constant section pile. Cao et al. [4] investigated the horizontal mechanical responses of a single pile and found that the horizontal displacements and bending moments of a single pile were controlled by the diameter, length, and elastic modulus of the pile. Zhou et al. [5] performed a group of field tests to study the influence of soil reinforcement along the pile shaft of a pre-stressed high-strength concrete (PHC) pile on the uplift bearing capacity of the pile. The results indicated that the ultimate skin friction of the PHC pile could be improved greatly in comparison to the pile with a cemented soil-soil interface. Franza et al. [6] proposed a two-stage model to characterize the influence of external actions and ultimate pile shaft stresses on the response of a pile group that was subjected to vertical and tunnelling-

induced loads, which can estimate both pile displacements and internal forces. Lueprasert et al. [7] investigated the influence of pile under loading on its adjacent tunnel, and the soil–pile interaction mechanism behind tunnel response was elucidated by a numerical simulation method. Wang et al. [8] found that pile diameter and bending stiffness have significant effects on load transfer curves ( $p$ – $y$  curves) of laterally loaded monopiles in dense sand, and a new  $p$ – $y$  curve that can account for the failure mechanism of large-diameter monopile was proposed. Wu and Vanapalli [9] found that a decrease in suction resulted from water infiltration led to different results compared with the widely accepted behavior of a single pile in unsaturated expansive soils. The effect of suction on the rational pile foundation designed in expansive soils should be taken into consideration. Wang and Ishihara [10] derived a semi-analytical model that could accurately predict the load–displacement curves and moment response for the pile foundations with multiple pile diameters and aspect ratios. Nakagama et al. [11] demonstrated that the mechanism of subgrade reaction of grouped pile in dry ground is remarkably different from that in saturated ground.

Moreover, it is commonly accepted that the research findings in the variable section pile are much less than those in the constant section pile. The investigation into the variable section pile mainly focuses on its bearing mechanism. Li et al. [12, 13] revealed the migration patterns of sand particles around the piles with footing and bucket. They considered that the footing and bucket could improve the efficiency of soil stress mobilization at shallow depth, and that pile–footing foundation and pile–bucket foundation provide better performance in lateral response. Shen et al. [14] developed a theoretical method to predict the uplift capacities of helical piles with a single plate, which could take the installation speed and the out diameter of the helix into consideration. Fayez et al. [15], based on a large-scale shark table testing system to study the dynamic response of single and grouped helical piles to seismic load, considered that the maximum shear force and the maximum bending moment occurred when the helical pile in a group was moving away from the softened soil zone. Harnish and Hesham El Naggar [16] carried out a series of field pile load tests to determine the interpreted ultimate capacity of the test helical piles, considering that the installation torque had a significant influence on the large-diameter helical pile capacity. Li et al. [17] employed a 3D nonlinear dynamic numerical simulation method to explore the effectiveness of X cross-sections in mitigating slope displacements, suggesting that the lateral slope displacements would be significantly reduced by X-shaped pile groups compared with circle pile-improved ground, and that the deformation response would be controlled by the spacing, pile orientation, and pile fixity. Additionally, the squeezed branch pile has attracted the attention of numerical scholars for its superior bearing performance. Shi et al. [18] comparatively analyzed the difference in stress characteristics and applicable scope between two kinds of squeezed branch piles formed by unidirectional squeezed workmanship and bidirectional squeezed workmanship. Zhang et al. [19] numerically analyzed the influence of branch position, spacing, number,

and diameter on the bearing capacity of the squeezed pile, considering that the pile top load would be shared by branches, and that the squeezed branch pile had two different failure mechanisms, named the individual branch failure mechanism and the cylindrical failure mechanism. Liu et al. [20] established and verified a calculation method based on the load transfer method to calculate the bearing capacity of a squeezed branch pile and found that the dependence of settlement on resistance could be described by the hyperbolic function to reveal the nonlinear property of the interaction between soil and pile, and the bearing capacity of the squeezed pile mainly depends on the bearing capacity of branch and pile end compared to the contribution of pile-side friction to the bearing capacity of the squeezed pile. Ma et al. [21] proposed a calculation theory of squeezed branch piles based on the shear displacement method, finding that the theoretical bearing capacity of the squeezed branch pile agreed well with experimental results. Wang et al. [22] carried out a static load test to systematically study the bearing capacity of a squeezed branch pile, which suggested that the branch could effectively reduce the pile shaft axis force and greatly reduce the pile end shaft force, leading to a slow change trend in load–displacement curves of the squeezed piles compared with that of the constant section piles. Al-Suhaily et al. [23] designed a pile with an enlarged base that consisted of a pile shaft with a square section and two or four open-ended gates from the sides of the pile shaft. They found that the gates could increase the bearing area and further increase the bearing capacity of a pile. Al-Shakarchi et al. [24] conducted laboratory experiments to investigate the influence of uplift loads with various inclinations on the uplift capacity of a batter pile. They considered that the uplift capacity of a vertical or batter pile was proportional to the inclination of pullout loading, and a greater uplift load belonged to a negative batter pile rather than a positive batter pile under all the loading inclinations.

In this paper, a new type of squeezed multiple-branch pile is proposed. The forming tool of the squeezed branch is invented, which is authorized by the China National Intellectual Property Administration with a patent number: ZL 201710377924.7. The effect of branch spacing and number on pile uplift bearing capacity was examined using numerical simulation software called FLAC3D on a total of 11 piles, 10 of which had squeezed multiple branches and one of which had a constant section. The dependence of the load–displacement curves, ultimate uplift bearing capacity, side friction resistance, stress distribution law in the pile, and the soil around the pile on the spacing and number of the branches was systematically analyzed from multiple perspectives.

## 2. New Squeezed Multiple-Branch Pile and Its Forming Tool

The new squeezed multiple-branch pile has a small branch diameter (branch diameter is less than two times the diameter of the pile with constant cross-section), which can be set up with several to a dozen branches depending on the length of the pile or the requirements of the single pile bearing

capacity. A forming device for the branch is invented and is reasonable in structure, light in weight, and fast in construction. The forming device does not easily trap soil in the process of preparing the branch. Moreover, the propulsion cavity can be retracted smoothly after repeated squeezing, which facilitates the free movement of the whole device in the borehole. In addition, the device is widely used, not easily affected by the working environment, and does not require special waterproof sealing treatment.

As shown in Figure 1(a), the new squeezed multiple-branch pile is made up of the squeezed branches 1 and pile shaft 2 with a circular cross-section. From Figures 1(b), 1(c), and 1(d), the forming device of the branch consists of a lower steel casing 3, an upper casing 4, casing support plate 5, oil inlet pipe 6, upper extension rod 7, oil return pipe 8, valve chamber 9, hinge 10, propulsion chamber 11, lower extension rod 12, hydraulic jack connecting block 13, inlet of oil return pipe 14, hydraulic jack 15, outlet of oil return pipe 16, and returning spring 17. The hydraulic jack is used for pushing the squeezing cavity to acquire the branches with a uniform thickness. The squeezing cavity can be smoothly returned when squeezing many times. To form the squeezed branch at one time, the flap cavity is added at 1/3 of the propulsion cavity. The forming device solves the disadvantage of the traditional squeezing device that is easy to pinch soil, with the advantage of being light in weight, easy to operate, and fast in construction. The forming device is equipped with steel casings and a semi-closed expansion cavity. The steel casings are close to the hole-wall to avoid the occurrence of soil collapse when the expansion cavity expands the soil.

### 3. Numerical Molding

In this paper, FLAC3D numerical simulation software was used to establish five groups of squeezed multiple-branch pile models with branch spacing of  $2.0d$ ,  $2.5d$ ,  $3.0d$ ,  $3.5d$ , and  $4.0d$  ( $d$  was the pile diameter), respectively, and one group of equal-section pile models, exploring the effect of the branch spacing on the uplift bearing capacity of the squeezed branch pile. Similarly, the pile models with branch numbers of 3, 4, 5, 6, and 7 were built. The branch spacing was 3.0 times of the pile diameter for the piles with branch numbers of 3, 4, and 5, whereas the branch spacing of the piles with branch numbers of 6 and 7, respectively, was 2.5 times and 2.0 times of the pile diameter. The contact surface was established between the pile and soil when modeling. Only one type of soil was selected as plain soil to exclude as much as possible the interference factors, exploring the effect of branch spacing and number on the uplift bearing capacity of the squeezed multiple-branch piles. The 1/4 model was selected for calculation because of the symmetrical geometry of the model, as shown in Figure 2. The parameters of the soil and pile are shown in Table 1.

The model size is  $15\text{ m (thickness)} \times 6\text{ m (width)} \times 6\text{ m (length)}$ . The pile length, pile diameter, and branch diameter are 10 m, 0.6 m, and 1.2 m, respectively. Brick elements are used to model soil mass and pile body. The construction technology of a squeezed branch pile is to use concrete,

and the rigidity of concrete is far greater than that of soil. Hence, the Mohr–Coulomb model is selected as the material model of soil mass, whereas the linear elastic constitutive model is used to simulate pile. The interaction between pile and soil is transferred through the establishment of a contact surface. Because the model is a typical axisymmetric body (geometric size symmetry, load symmetry), a quarter of the model is selected for simulation calculation. According to the axisymmetric plane problem of the half-space body in elastic mechanics, the vertical displacement of the soil below the boundary of the soil is assumed to be zero, that is, the vertical displacement of the soil at a certain depth from the bottom of the branch pile is zero. The depth of the soil below the bottom of the new squeezed multiple-branch pile is generally  $(8 \sim 10)d$  ( $d$  is the pile diameter), which is taken as 5 m in this paper. The unbalanced stress reached  $1 \times 10^{-6}$  as the end condition of the calculation to obtain sufficiently accurate results. The model did not have any sharp corner parts, and the singular stiffness matrix led to non-convergence. The uplift load was applied at the top of the pile starting from 200 kN (surface load, same below), and the load was increased by 200 kN per stage to a maximum loading of 5000 kN.

## 4. Numerical Simulation Results and Discussion

**4.1. Effect of Branch Spacing on Bearing Mechanism.** According to the load-settlement curves shown in Figure 3, it is judged that the ultimate uplift bearing capacity of the equal-section pile is 1000 kN, and the ultimate uplift bearing capacity of the piles with branch spacing of  $2.0d$ ,  $2.5d$ ,  $3.0d$ ,  $3.5d$ , and  $4.0d$  is 3400 kN, 4000 kN, 4200 kN, 3200 kN, and 2800 kN, respectively. The ultimate uplift bearing capacity of the new squeezed multiple-branch pile is significantly greater than that of the equal-section pile [22]. The branch spacing of  $3.0d$  is the dividing point of the load-settlement curve types (steep-declining style and slow-declining style). As shown in Figure 4, when the applied load  $\leq 1000\text{ kN}\cdot\text{m}^{-2}$ , the uplift settlements of the piles were basically the same, whereas the uplift settlements of piles were very different when the applied load  $> 1000\text{ kN}$ . The pile with branch spacing of  $3.0d$  has the most uniform increment of the uplift settlement, leading to the latest appearance of the uplift failure characteristics. It can be judged that the ultimate uplift bearing capacity of the new squeezed multiple-branch pile with a disc spacing of  $3.0d$  is the maximum. The reasons behind this phenomenon might be that the stress superposition range of the soil around the pile with branch spacing of  $L = 2.0d$ ,  $L = 2.5d$ , and  $L = 3.0d$  was gradually decreasing, and the reaction forces of the soil on the branches were gradually increasing, which led to the increasing ultimate uplift bearing capacity, while only part of the soil between the branches played a better role in the uplift bearing capacity for the pile with the branch spacing of  $L = 3.5d$  and  $L = 4.0d$ , leading to a decreased trend in the ultimate bearing capacity.

Figure 5(a) displays the diagram of the pullout failure mode of the squeezed multiple-branch pile, and the form of the sliding failure surface determines the uplift bearing

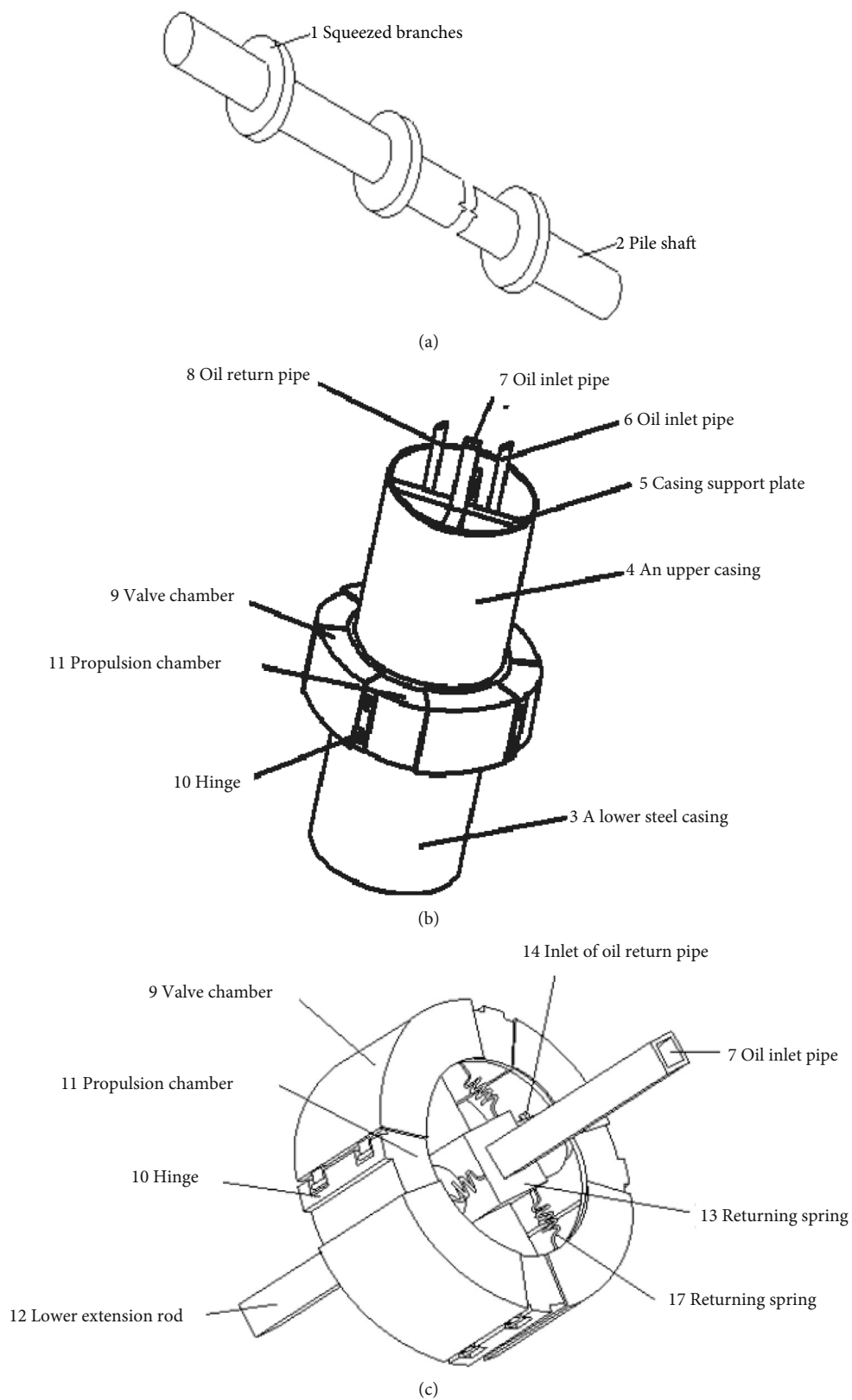


FIGURE 1: Continued.

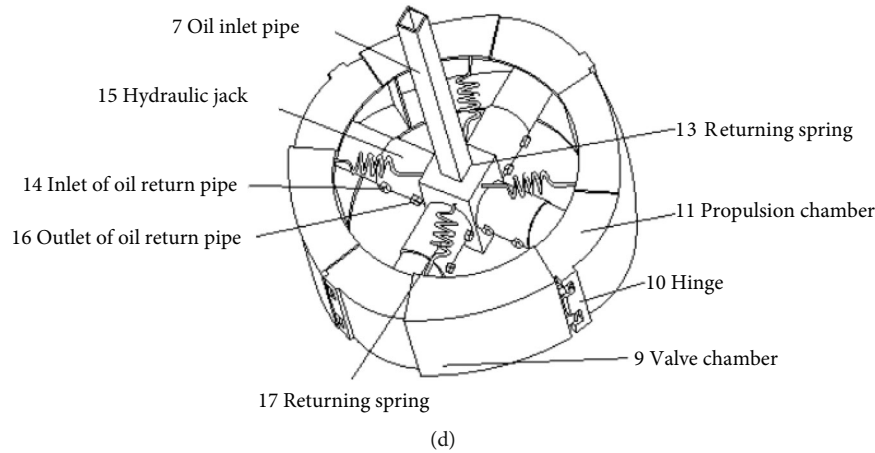


FIGURE 1: Schematic diagram of the structure of the forming tool: (a) new type of squeezed multiple-branch pile; (b) schematic diagram of the whole structure; (c) schematic diagram when the propelling cavity completes push-out; and (d) schematic diagram when the propelling cavity with valve cavity completes push-out.

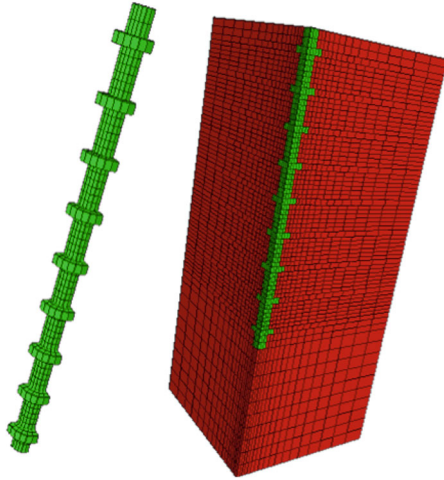


FIGURE 2: Computational model of FLAC3D.

capacity of the piles [25]. Figure 5(b) depicts the Z-direction displacement diagram of the pile with branch spacing of  $2.0d$  when loaded to 4000 kN, at which point the pile was damaged. The thin soil layer between the branches had insufficient bearing capacity, which caused shear failure in a through-going manner of the soil layers along the sliding plane of 1 and 2 in Figure 5(a). Figure 5(c) presents the contour of Z-displacement of the pile with branch spacing of  $2.5d$  when loaded to 4000 kN close to the ultimate bearing capacity. The soil layer between branches became thicker compared with that of the pile with branch spacing of  $2.0d$ , resulting in the shear failure mode along the sliding plane of 1 and 3 in the soil around the pile. However, most of the soil on the branches was shear failure pattern along the sliding plane of 3, whereas the sliding trend along the sliding plane of 4 was unapparent. As shown in Figure 5(d), the soil around the pile with branch spacing of  $3.0d$  was thick enough to support a main failure trajectory along the sliding plane of 3 and a subordinate failure trend along the sliding plane of 4.

Notably, the load of 4000 kN did not reach the bearing capacity of the pile with branch spacing of  $3.0d$ . Figures 5(e) and 5(f) displayed the contour of Z-displacement of the pile with branch spacing of  $3.5d$  and  $4.0d$  when loaded to 4000 kN, with large soil displacement between branches within  $3.0d$ . Namely, the soil within  $3.0d$  from the upper surface of the branches performed a partial penetration shear failure pattern along a sliding plane of 1 with an increased distribution of the plastic zone of the soil, leading to a decrease in bearing capacity compared with the pile with the other branch diameters. The statement about the phenomenon of the pile with branch spacing of  $4.0d$  was more obvious than that of the pile with branch spacing of  $3.5d$ . It can be determined that the ultimate uplift bearing capacity of the new squeezed multiple-branch pile with branch spacing of  $3.0d$  was the largest. From the displacement diagram of the pile with branch spacing of  $3.0d$ , the spread scope of displacement in X-direction is about three times of the branch diameter from the centerline of the pile, and considering the effect of group pile, this paper considered that the minimum center distance between the uplift resistant piles in the group pile was six times of the branch diameter.

**4.2. Effect of Branch Number on Bearing Mechanism.** The uplift load was applied to the top surface of the new squeezed multiple-branch pile, starting from 1600 kN up to 5000 kN and loading 200 kN per stage. According to the load-displacement curves, as shown in Figure 6, the ultimate uplift bearing capacity of the pile with the branch numbers of 3, 4, 5, 6, and 7 was judged to be 3400 kN, 3800 kN, 4200 kN, 4000 kN, and 3400 kN, respectively. Namely, although the pile with branch number of 6 had the smallest uplift displacement before reaching its ultimate bearing capacity, it reached the ultimate uplift capacity before the pile with support plate number 5, so the pile with support plate number 5 has the largest ultimate uplift capacity. When the number of branches was less than 5, the uplift displacement decreased with the increase in the number of



TABLE 1: Parameters of soil and pile.

	Bulk modulus (Pa)	Shear modulus (Pa)	Density ( $\text{kg}\cdot\text{m}^{-3}$ )	Cohesion (Pa)	Internal friction angle ( $^\circ$ )
Plane soil	$4.4 \times 10^7$	$2.0 \times 10^7$	$1.6 \times 10^3$	$8.0 \times 10^3$	24.0
Pile	$3.0 \times 10^{10}$	$1.9 \times 10^9$	$2.5 \times 10^3$	—	—

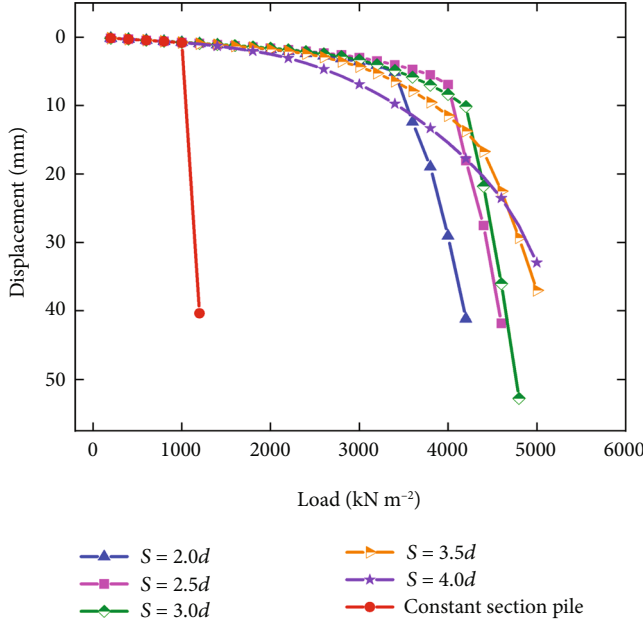
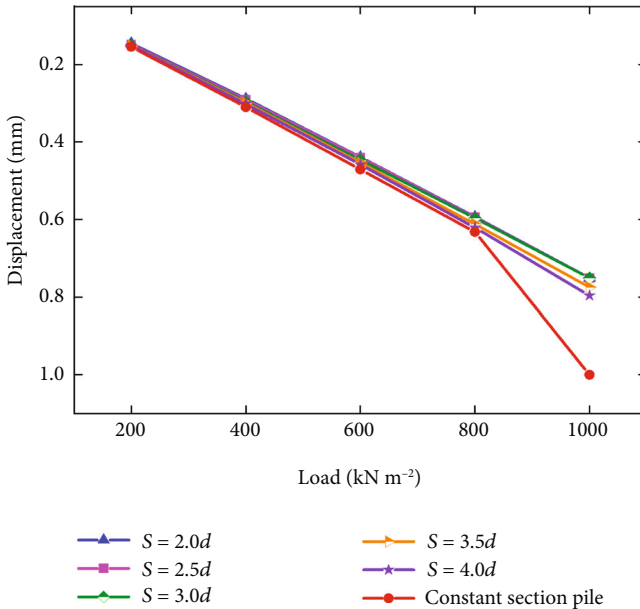


FIGURE 3: Load-displacement curves.

FIGURE 4: Load-displacement curves when the load  $\leq 1000$  kN.

branches. The volume of the effective bearing soil body in the shape of an inverted circular table on the branches gradually increased, which made the load-displacement curves gradually change from steep-decreasing type to a slow-varying type. This indicated that the function of the effectively

pressurized soil between the branches was gradually enhanced, making the bearing advantage of the branches gradually apparent. When the number of supporting discs was greater than 5, all the load-displacement curves were transformed into steep-declining types. As shown in Figure 7, the increase in the ultimate uplift bearing capacity of the pile with a number of branches greater than 5 was greater than that of the pile with a number of branches less than 5. The ultimate uplift bearing capacity was linearly increased with branch number from 3 to 5, which was completely opposed to that of the pile with branch number from 5 to 7.

The pile with a branch number of 5 was employed to describe the influence of branches on axial force of pile shaft ( $F_1$ ) and pile-side friction resistance, and the rest of the new squeezed multiple-branch piles were similar to it. The axial force dropped steeply at the position of the branch, with a remarkable branch bearing effect, as shown in Figure 8. Except for the top branch (i.e., branch 1), the load shared by each plate increased linearly when the uplift load was more than 2000 kN, but the load shared by each branch was similar when the uplift load was less than 2000 kN, as displayed by Figure 9. As the load increased, the load shared by each branch ( $F_2$ ) was directly proportional to the depth of the branch, which was an obvious difference compared to the constant section pile. Due to the thin thickness of the soil on the branch 1, it could not provide enough resistance to make the branch play its bearing advantage, resulting in a stable state for the shared load by branch 1.

The load sharing ratio  $\eta$  is the ratio of the sum of the loads borne by the branches to the ultimate bearing capacity of the squeezed multiple-branch pile. As presented in Figure 10, the load sharing ratio of the branches was within the range of 40%–70%, and the sum of the load shared by the pile with branch number of 5 had the lowest proportion but also shared nearly 50% of the total uplift load. The load increment borne by each branch of the pile with a branch number of 5 was the most gentle, which implied that the stress concentration in the branch of the pile was much smaller than that of the other piles with various branches, and the pile with branch number of 5 had more safety reserves. The sum of the loads borne by the branches tended to stabilize when the piles with branch numbers of 4 and 5 were close to the uplift limit bearing capacity, while the sum of the loads borne by the other piles with multiple branches showed a decreasing tendency. This indicated that the soil on one or several branches had a through shear damage state, so a pile with a branch number of 5 was reasonable. As shown in Figure 11, the pile lateral frictional resistance is closely related to the branch number. In general, the pile-side frictional resistance of a pile with a branch number of 5 was the best and stabilized at the later stage of loading, indicating that the pile with a branch number

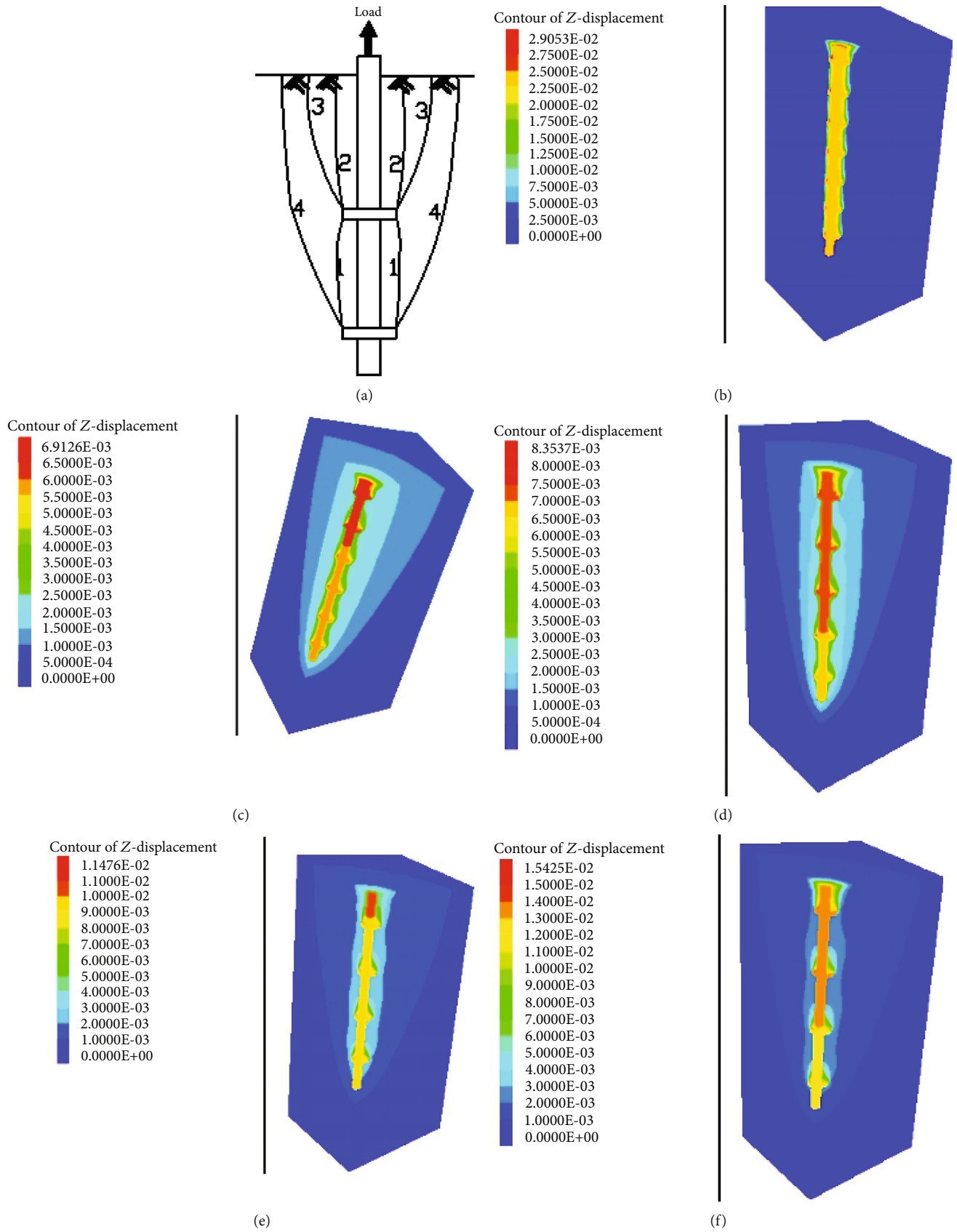


FIGURE 5: Failure patterns schematic and displacement contours: (a) pullout failure mode of pile, (b) contour of Z-displacement when  $S = 2.0d$ , (c) contour of Z-displacement when  $S = 2.5d$ , (d) contour of Z-displacement when  $S = 3.0d$ , (e) contour of Z-displacement when  $S = 3.5d$ , and (f) contour of Z-displacement when  $S = 4.0d$ .

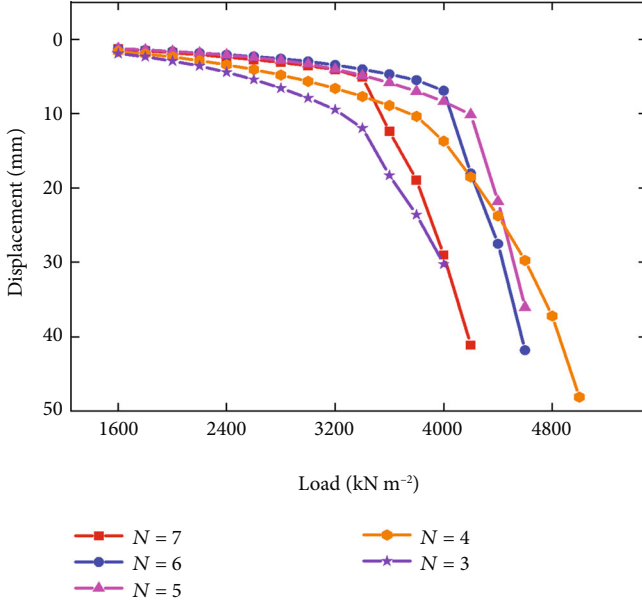


FIGURE 6: Load-displacement curves of pile with various branches.

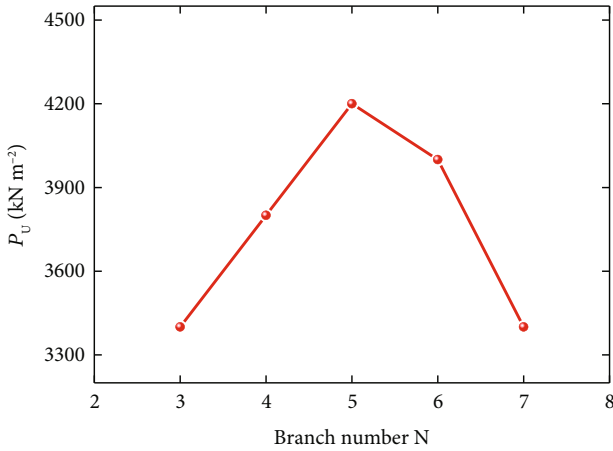


FIGURE 7: Relationship between ultimate uplift bearing capacity and branch number.

of 5 could maximize the bearing effect of soil on branches. From Figures 10 and 11, there was an obvious complementary relationship between the bearing force of the branches and the lateral frictional resistance of the pile for the new squeezed multiple-branch pile.

The stress state of the soil around the pile can indirectly reflect the state of the support plate bearing force and the degree of pile lateral frictional resistance, as displayed in Figure 12. That was the distribution of principal stresses in piles with various branch numbers when loaded to 4000 kN. Concentrated tensile and compressive stresses appeared at the root of the upper surface and the root of the lower surface of the branches, respectively. The degree of stress concentration gradually increased from top to bottom, i.e., the load borne by the branches gradually increased from top to bottom, which was the unique bearing feature of

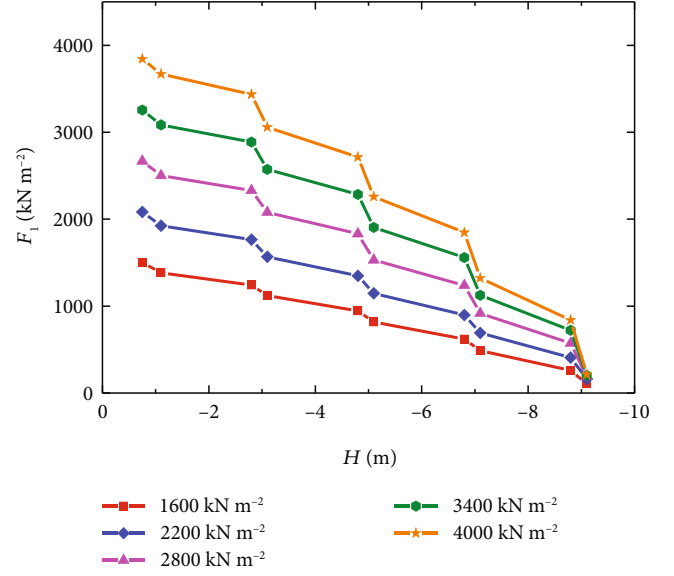


FIGURE 8: Distribution map of axial force of pile.

the new squeezed multiple-branch pile. Hence, it is important to ensure the quality of concrete placement in the actual project, so that the pile will not suffer from tensile damage due to the poor tensile properties of concrete. The degree of stress concentration in the soil between branches was inversely proportional to the number of branches. The greater the number of branches, the lower the possibility of shear damage of the branch itself, and the highest safety reserve of the branch, but its ultimate pullout resistance was not the highest.

Moreover, a gradually decreasing stress bubble was formed on the upper surface of the branch, and the stress distribution in the soil body presented a parabolic pattern spreading outward, which was consistent with the actual situation. For the five kinds of piles with different numbers of branches, the soil immediately below the surface of the branches showed areas of stress close to 0 (zero-stress zone) but to a small extent. When the number of branches was less than 5, the range of zero-stress zone was inversely proportional to the burial depth of the branch and the number of branches, which meant that the soil under the branch had been separated from the branch, and the load at this time was very close to the ultimate uplift bearing capacity, but the range of zero-stress zone of 5 disc piles was the smallest, so the ultimate uplift bearing capacity of 5 disc piles was greater than that of piles with branch numbers of 3 and 4. When the number of discs was greater than 5, the range of the zero-stress zone was larger than that of the piles with the number of branches less than 5. And, because the range of the zero-stress zone was proportional to the number of branches, with a greater tendency for through shear damage, the ultimate uplift bearing capacity of a pile with a branch number of 5 was greater than that of piles with branch numbers of 6 and 7.

Additionally, the stress diffusion of the soil around the new squeezed multiple-branch pile all appeared for the pile with various branch numbers, and the stress diffusion range



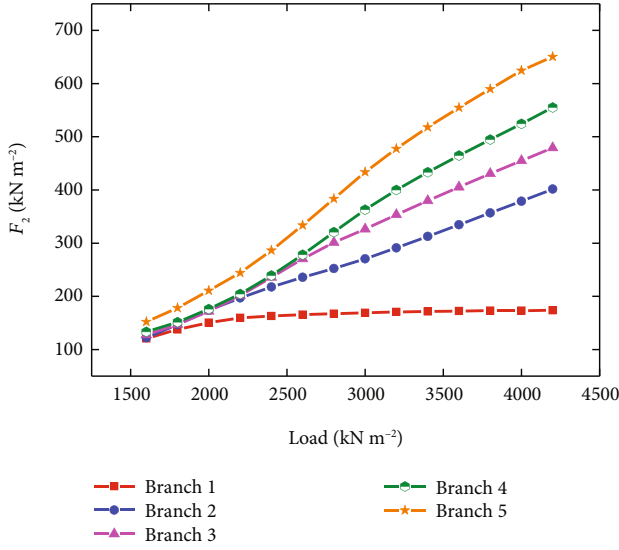


FIGURE 9: Load sharing per branch.

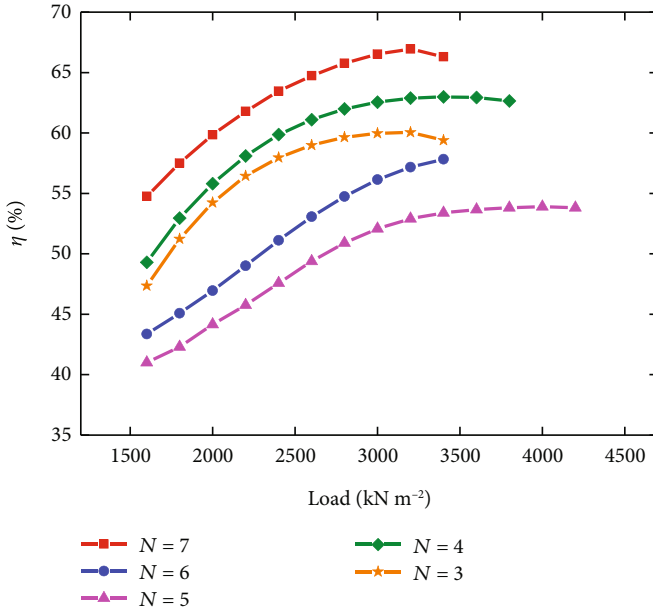


FIGURE 10: Relationship between the load ratio and the branch number.

of the soil on the upper surface of the branch was larger than that of the soil at the lower part of the branch. The extent of stress diffusion in the soil was inversely proportional to the burial depth of the branch and the number of branches. For the piles with a number of branches less than 5, the stress superposition was already very obvious, and the plastic zone of the soil around the pile had been penetrated, leading to the failure of the pile bearing effect and the steeply increased uplift displacement. The stress superposition of the pile with a branch number of 5 was much smaller than that of the piles with branch numbers of 3 and 4, and there was no through-shear damage in the soil around the pile, so the pile with branch number of 5 had the largest ultimate uplift bearing capacity.

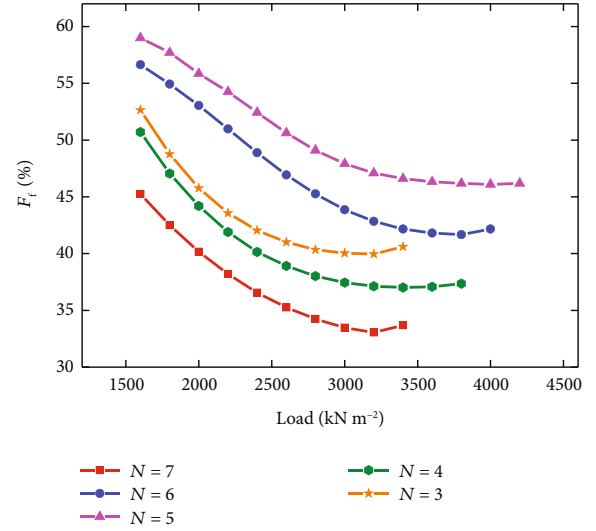


FIGURE 11: Relationship between pile-side friction ratio and branch number.

## 5. Conclusions

A new squeezed multiple-branch pile was proposed to investigate the effects of branch spacing and branch number on uplift bearing capacity, load-displacement curves, branch bearing mechanism, pile-side friction resistance, and principle stress distribution law under uplift load. The primary conclusions could be summarized as follows:

- (1) Under the same conditions, the ultimate uplift capacity of the new squeezed multiple-branch pile was about four times that of equal-section pile. In the plain soil, the pile with a branch spacing of about 3.0 times the pile diameter was the largest. On this basis, the pile length, pile diameter, and branch number could be adjusted according to the mechanical properties of the soil layer.
- (2) The ultimate uplift bearing capacity of the new squeezed multiple-branch pile was the largest when the branch number was 5. The pile-side friction resistance mainly played a major role in the early stage of loading, and the bearing advantage of the branches was mainly highlighted in the later stage. The load sharing ratio of the branches was within the range of 40–70%, and the deeper the support plate was buried, the greater the load sharing.
- (3) Concentrated tensile stresses and concentrated compressive stresses appear at the root of the upper surface of the branch and the root of the lower surface of the branch, respectively. And concentrated compressive stresses occurred at the connection part with the pile body. It was important to ensure the quality of concrete placement in the actual project to avoid tensile failure of the pile for the poor tensile properties of concrete.
- (4) When the number of branches was less than 5, the range of the zero-stress zone was inversely proportional to the burial depth of the branch and the number of branches. When the number of branches was

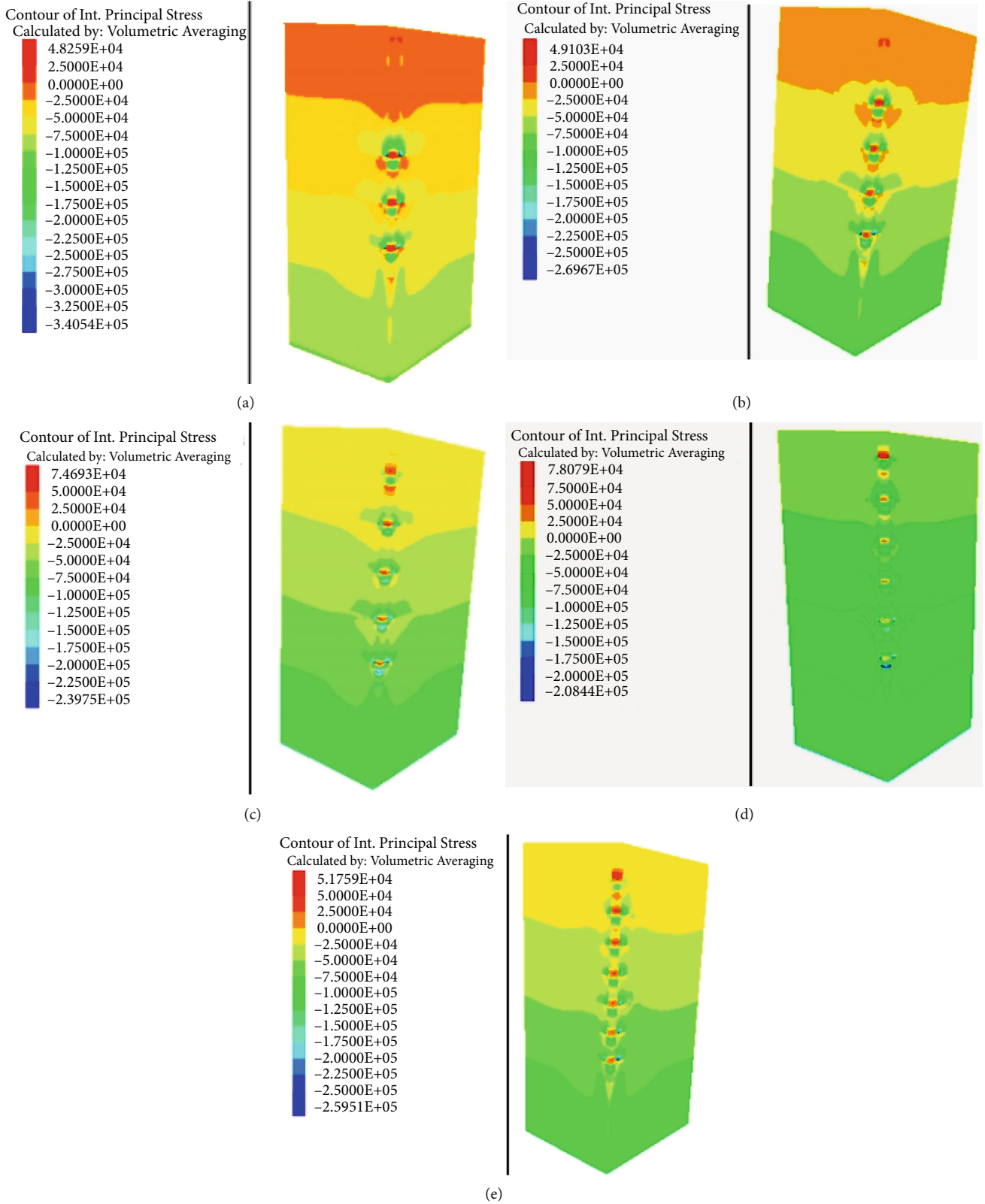


FIGURE 12: Distribution diagram of main stress of pile with various branches: (a) pile with branch number of 3, (b) pile with branch number of 4, (c) pile with branch number of 5, (d) pile with branch number of 6, and (e) pile with branch number of 7.

greater than 5, the range of the zero-stress zone was larger than that of the piles with a branch number of less than 5, and the more branches, the larger the range of the zero-stress zone.

## Data Availability

The datasets generated and analyzed during the current study are available from the corresponding author on reasonable request.

## Conflicts of Interest

The authors declare that they have no conflicts of interest.

## Acknowledgments

This research receives financial supports by the Open Foundation of Anhui Province Key Laboratory of Building Structure and Underground Engineering (No. KLBSUE-2020-04), Anhui Jianzhu University, Hefei. Thanks to West Anhui University and Anhui University of Science and Technology for providing the research conditions.

## References

- [1] W. O. McCarron, "Efficient analysis of cyclic laterally loaded piles," *Results in Engineering*, vol. 10, p. 100213, 2021.
- [2] Y. Shao, W. Xiao, K. Xiang, B. Wang, and S. Zhou, "Semi-automatic construction of pile-supported subgrade adjacent to existing railway," *Automation in Construction*, vol. 134, p. 104085, 2022.
- [3] M. K. Pradhan, P. Kumar, V. S. Phanikanth, D. Choudhury, and K. Srinivas, "A review on design aspects and behavioral studies of pile foundations in liquefiable soil," *Geomechanics and Geoengineering*, vol. 2022, pp. 1–33, 2022.
- [4] L. Cao, D. Zhang, X. Shen, S. Jie, H. Fang, and S. Dong, "Horizontal mechanical responses of single pile due to urban tunnelling in multi-layered soils," *Computers and Geotechnics*, vol. 135, p. 104164, 2021.
- [5] J. Zhou, Y. Jianlin, X. Gong, R. Zhang, and T. Yan, "Influence of soil reinforcement on the uplift bearing capacity of a pre-stressed high-strength concrete pile embedded in clayey soil," *Soils and Foundations*, vol. 59, no. 6, pp. 2367–2375, 2019.
- [6] A. Franza, C. Zheng, A. M. Marshall, and R. Jimenez, "Investigation of soil-pile-structure interaction induced by vertical loads and tunnelling," *Computers and Geotechnics*, vol. 139, p. 104386, 2021.
- [7] P. Lueprasert, P. Jongpradist, P. Jongpradist, and S. Suwansawat, "Numerical investigation of tunnel deformation due to adjacent loaded pile and pile-soil-tunnel interaction," *Tunnelling and Underground Space Technology*, vol. 70, pp. 166–181, 2017.
- [8] H. Wang, L. Z. Wang, Y. Hong, B. He, and R. H. Zhu, "Quantifying the influence of pile diameter on the load transfer curves of laterally loaded monopile in sand," *Applied Ocean Research*, vol. 101, p. 102196, 2020.
- [9] X. Y. Wu and S. K. Vanapalli, "Three-dimensional modeling of the mechanical behavior of a single pile in unsaturated expansive soils during infiltration," *Computers and Geotechnics*, vol. 145, p. 104696, 2022.
- [10] L. Wang and T. Ishihara, "A semi-analytical one-dimensional model for offshore pile foundations considering effects of pile diameter and aspect ratio," *Ocean Engineering*, vol. 250, p. 110874, 2013.
- [11] Y. Nakagama, Y. Tamari, H. Yoshida, M. Yamamoto, and H. Suzuki, "Numerical analysis on seismic behavior of soil around pile group by 3D effective stress finite element method," *Soils and Foundations*, vol. 62, no. 2, p. 101123, 2022.
- [12] L. Li, M. Zheng, X. Liu et al., "Numerical analysis of the cyclic loading behavior of monopile and hybrid pile foundation," *Computers and Geotechnics*, vol. 144, p. 104635, 2022.
- [13] L. Li, H. Liu, W. Wu, M. Wen, M. H. E. Naggar, and Y. Yang, "Investigation on the behavior of hybrid pile foundation and its surrounding soil during cyclic lateral loading," *Ocean Engineering*, vol. 240, p. 110006, 2021.
- [14] B. Shen, O. Stephansson, H. H. Einstein, and B. Ghahreman, "The uplift capacity of single-plate helical pile in shallow dense sand including the influence of installation," *Marine Structures*, vol. 71, p. 102697, 2019.
- [15] A. F. Fayed, M. H. El Naggar, A. B. Cerato, and A. Elgama, "Seismic response of helical pile groups from shake table experiments," *Soil Dynamics and Earthquake Engineering*, vol. 152, p. 107008, 2021.
- [16] J. Harnish and M. Hesham El Naggar, "Large-diameter helical pile capacity-torque correlations," *Canadian Geotechnical Journal*, vol. 54, pp. 968–986, 2017.
- [17] W. Li, A. W. Stuedlein, Y. Chen, H. Liu, and Z. Cheng, "Response of pile groups with X and circular cross-sections subject to lateral spreading: 3D numerical simulations," *Soil Dynamics and Earthquake Engineering*, vol. 126, p. 105774, 2019.
- [18] S. Dequan, X. Jian, Y. Chun, and L. Baolin, "Research on the plate cavity geometry of the squeezed branch pile," *Procedia Engineering*, vol. 73, pp. 29–34, 2014.
- [19] M. Zhang, X. Ping, W. Cui, and Y. Gao, "Bearing behavior and failure mechanism of squeezed branch piles," *Journal of Rock Mechanics and Geotechnical Engineering*, vol. 10, no. 5, pp. 935–946, 2018.
- [20] L. Liu, H. Ma, X. Yang, Q. He, and S. Yuan, "A calculation method of bearing capacity of single squeezed branch pile based on load transfer method," *Advances in Materials Science and Engineering*, vol. 2022, p. 9597047, 2022.
- [21] L. N. Y. Wong and H. H. Einstein, "Research on bearing theory of squeezed branch pile," *Advances in Civil Engineering*, vol. 2020, pp. 1–12, 2020.
- [22] L. Li, X. Li, X. Cheng, and H. Huang, "Load transfer method for squeezed and branch piles considering cavity expansion theory," *China Journal of Highway and Transport*, vol. 31, pp. 20–29, 2018.
- [23] A. S. Al-Suhaily, A. S. Abood, and M. Y. Fattah, "Bearing capacity of uplift piles with end gates," *Proceedings of China-Europe Conference on Geotechnical Engineering*, pp. 893–897, 2018.
- [24] Y. J. Al-Shakarchi, M. Y. Fattah, and I. K. Kashat, "The behaviour of batter piles under uplift loads," *International Conference on Geotechnical Engineering*, pp. 105–114, Sharjah University, Sharjah – UAE, 2004.
- [25] Z. Baodian and L. Chengyuan, "Study on uplift mechanism and engineering application of disk piles," *Architecture Technology*, vol. 40, pp. 843–846, 2009.